

Article

Not peer-reviewed version

# The Influence of Codon Optimization on the Immune Response and Protective Efficacy of DNA Vaccines based on the Dengue Envelope and NS1 Proteins

[Simone Morais Costa](#) <sup>\*</sup>, Ágatha Rezende Pacheco, Paolla Beatriz Almeida Pinto, Maysa Leandro Assis, Pedro Rasch, Rafael L.C. Silva, Márcio Mantuano Barradas, [Ada Maria de Barcelos Alves](#) <sup>\*</sup>

Posted Date: 15 November 2023

doi: 10.20944/preprints202311.1032.v1

Keywords: DNA vaccine; dengue; codon-optimization; envelope and NS1



Preprints.org is a free multidiscipline platform providing preprint service that is dedicated to making early versions of research outputs permanently available and citable. Preprints posted at Preprints.org appear in Web of Science, Crossref, Google Scholar, Scilit, Europe PMC.

Copyright: This is an open access article distributed under the Creative Commons Attribution License which permits unrestricted use, distribution, and reproduction in any medium, provided the original work is properly cited.

## Article

# The Influence of Codon Optimization on the Immune Response and Protective Efficacy of DNA Vaccines based on the Dengue Envelope and NS1 Proteins

Simone M. Costa <sup>1,\*</sup>, Ágatha R. Pacheco <sup>1</sup>, Paolla B. A. Pinto <sup>1</sup>, Maysa L. Assis, Pedro Rasch <sup>1</sup>, Rafael L. C. Silva <sup>1</sup>, Márcio M. Barradas <sup>2</sup> and Ada M.B. Alves <sup>1,\*</sup>

<sup>1</sup> Laboratory of Biotechnology and Physiology of Viral Infections, Oswaldo Cruz Institute, Fiocruz, Rio de Janeiro, RJ, Brazil; agatha.arp@gmail.com (Á.R.P.); paollabap@gmail.com (P.B.A.P.); pedrorasch@gmail.com (P.R.); rcorrea@id.uff.br (R.L.C.S.)

<sup>2</sup> Trypanosomatid Biochemistry Laboratory, Oswaldo Cruz Institute, Fiocruz, Rio de Janeiro, RJ, Brazil; marcio.mantuano@ioc.fiocruz.br

\* Correspondence: simonemc@ioc.fiocruz.br (S.M.C.); ada@ioc.fiocruz.br (A.M.B.A.)

**Abstract:** Dengue is a pan-tropical arthropod-borne disease, endemic in over 100 countries. The dengue virus comprises four antigenic serotypes (DENV 1-4). The envelope (E) and non-structural 1 (NS1) proteins are highly immunogenic, and the E protein carries epitopes eliciting neutralizing antibodies. In previous studies, mice immunizations with two DNA vaccines encoding the E ectodomain (pE1D2) and NS1 proteins (pcTPANS1) from DENV2 induced high protection. Based on these findings, we constructed new plasmids containing the codon-optimized genes from these proteins for expression in mouse and human cells, named pEotmD2 and pNS1otmD2. Compared to the pE1D2, the pEotmD2 mediated lower expression of the recombinant protein in human and mouse cell lines, while the pNS1otmD2 plasmid was slightly more efficient than the pcTPANS1 in these cells. Immunogenicity and protection were evaluated in BALB/c mice immunized with the original and codon-optimized plasmids followed by the challenge with DENV2. In accordance with the in vitro experiments, the antibody response and protection elicited by the pE1otmD2 plasmid was lower than those observed with the pE1D2. In contrast, the pNS1otmD2 vaccine enabled slightly higher levels of the humoral and protective responses than the pcTPANS1. Overall, our study revealed different effects of codon optimization on these two dengue DNA vaccines.

**Keywords:** DNA vaccine; dengue; codon-optimization; envelope and NS1

## 1. Introduction

The worldwide occurrence of dengue has significantly increased in recent years, representing a potential risk to approximately half of the global population [1]. The World Health Organization established the goal of controlling dengue by 2030, achieving a 0% fatality rate [2]. The dengue virus (DENV) comprises four genetically related serotypes (DENV1-4), and is transmitted by *Aedes* (*Ae*) *aegypti* or *Ae. albopictus* mosquitoes [3]. This enveloped virus contains a single-stranded RNA genome which encodes the structural proteins, capsid (C), envelope (E) and premembrane/membrane (prM/M), as well as the non-structural proteins NS1, NS2A, NS2B, NS3, NS4A, NS4B and NS5 [4].

The DENV infection can vary from asymptomatic to a range of clinical presentations, encompassing oligosymptomatic forms to severe cases [5]. While infection with one DENV serotype induces long-lasting protective immunity against the infecting serotype, the probability of manifesting severe dengue is significantly increased in secondary infections with heterologous serotypes [6–8].

The advancement of a dengue vaccine has encountered various obstacles, with the main one being the construction of a vaccine that effectively protects against the four viral serotypes, with a

sustained efficacy and without the risk of vaccinated individuals manifesting severe dengue after contact with the virus [9,10]. There are currently two licensed dengue vaccines, Dengvaxia (Sanofi-Pasteur) and Qdenga (Takeda Pharmaceuticals). The Dengvaxia consists of four chimeric viruses composed of the yellow fever vaccine virus (YFV-17D) backbone and sequences encoding the prM and E proteins of the four DENV serotypes. Phase 3 trials showed that the vaccine efficacy and safety varied depending on the individual serological status, the DENV serotype and the age [11–13]. The implementation of this vaccine in endemic countries led to serious safety concerns since increased hospitalization risk was observed in dengue-naïve vaccines exposed to DENV. Currently, the vaccine is only recommended for individuals aged between 9 and 45 years, seropositive for dengue [13,14]. The Qdenga, which was licensed in 2022, consists of four chimeric viruses containing the attenuated DENV2 backbone in which the genes encoding the prM and E proteins were substituted by sequences from the other three DENV serotypes [15]. During the phase 3 trial conducted among children and adolescents residing in dengue-endemic regions across Asia and the Americas, the vaccine efficacy also varied depending on the recipient dengue serostatus and serotype, with greater efficacy for DENV2 [16].

All these results point out the need to develop other vaccine strategies against dengue. During the COVID-19 pandemic, nucleic acid vaccines were consolidated as an alternative to conventional vaccine platforms. RNA vaccines have been administered globally and the first DNA vaccine for use in humans against COVID-19 was recently licensed [17–19]. These vaccines induce broad-spectrum humoral and cellular immune responses. Although preclinical research in several animal models demonstrated the efficacy of the DNA vaccines, clinical studies revealed suboptimal immunogenicity generated by such vaccines. Thus, various approaches have been devised to increase the efficacy of DNA vaccines, including codon optimization of the specific genes according to the host species to amplify the *in vivo* recombinant protein production [18,20–22].

The E protein is the primary focus of dengue vaccines because of its role in the virus adhesion and entry into host cells, fusion of viral and cell membranes, and delivery of the virus RNA into cell cytoplasm [10,23–25]. This glycoprotein is structured in dimers, with each monomer comprising three domains (DI, DII and DIII), that together form the ectodomain, and a transmembrane domain, the stem and anchor region located in the C-terminal region [26,27]. The E protein plays an important role in the humoral response, mainly by inducing the production of neutralizing antibodies [25,28]. The NS1 protein elicits robust immune responses, stimulating humoral and cellular immune responses during viral infection [29,30]. This glycoprotein is found at the cellular membrane and is released as a hexamer from infected cells during the acute phase of the infection [31–34]. It plays a role in viral replication, acts in the evasion of the immune system and in some other aspects of dengue pathogenesis [35–38]. Several reports demonstrated the protective effect of NS1 and pointed it as an important antigen in the composition of a vaccine against dengue [14,39–43].

In prior studies, we developed two DNA vaccines containing the ectodomain of the E (pE1D2) sequence or the *ns1* (pTPANS1) gene from DENV2. Inoculation of these plasmids in mice elicited high protection levels against DENV2 challenge [40,44]. Considering that dengue proteins are naturally expressed in both mosquito and human cells, in the current study we aim to improve the efficacy of these DNA vaccines by increasing expression of the recombinant E and NS1 proteins in the mouse model used for testing the vaccines, as well as in humans for future clinical tests. For this purpose, we analyzed the efficiency of codon optimization of the DNA vaccines containing *e* (pEotmD2) and *ns1* (pNS1otmD2) genes from DENV2. Human and murine cells were transfected with these new plasmids or the original vaccines, pE1D2 and pTPANS1, to evaluate expression of the recombinant proteins in both systems. Mice were immunized with all these DNA vaccines, followed by the challenge with DENV2. In general, the codon-optimized pE1otmD2 plasmid was less efficient in mediating the envelope protein expression and eliciting neutralizing antibodies than the plasmid pE1D2. These results were also reflected in the survival and morbidity following viral challenge, in which the pEotmD2 demonstrated to be less protective. In turn, the codon optimized pNS1otmD2 plasmid mediated an increased expression of the recombinant protein NS1 and induced slightly higher antibody and protection levels compared to the pTPANS1 plasmid.

## 2. Materials and Methods

### 2.1. Dengue Virus and Cells

The NGC DENV2 (strain New Guinea C, GenBank NCBI, M29095) was utilized in mice challenge assays, whereas for plaque reduction neutralization tests (PRNT<sub>50</sub>) we used the DENV2 44/2 [45]. For the PRNT<sub>50</sub>, Vero cells (ATCC®, CCL-81) were maintained in medium 199 with Earle's salts (M199, Sigma) with 5% fetal bovine serum (FBS, Invitrogen), sodium bicarbonate (25 mg/mL), in the presence of gentamicin (0.04 mg/mL, Sigma) at 37 °C with 5% CO<sub>2</sub>. The in vitro expression evaluation of the recombinant E and NS1 proteins was performed in two different cell lines: mouse neuroblastoma, Neuro2A (ATCC®, CCL-131) and human hepatoma, HuH7 (cells were obtained from Dr. Da Poian, Leopoldo de Meis Institute of Medical Biochemistry, Federal University of Rio de Janeiro). The Neuro2A cells were cultivated in RPMI-1640 medium (Sigma) and HuH7 cells were maintained in Dulbecco's Modified Eagle Medium (DMEM, Sigma), both supplemented with 10% FBS at 37°C with 5% CO<sub>2</sub>.

### 2.2. Original pE1D2 and pcTPANS1 Plasmids

The construction of the DNA vaccines pE1D2 and pcTPANS1 was previously described [40,44]. Briefly, the pE1D2 vaccine contains 80% of the *e* gene (sequence which encodes the ectodomain of the envelope protein) from DENV2, and the pcTPANS1 contains the DENV2 *ns1* gene. For secretion of the recombinant proteins, the genes were fused to the human tissue plasminogen activator signal peptide (t-PA) sequence. The plasmid pcTPA, containing only the t-PA sequence, was used as a negative control.

### 2.3. Construction of the Codon Optimized pEotmD2 and pNS1otmD2 Plasmids

To increase expression of the envelope (the ectodomain) and NS1 DENV2 proteins, the *e* and *ns1* genes, as well as the t-PA sequence, were codon optimized for expression in mouse and human cells (GenScript Biotech). Optimization was performed by reducing codon frequencies that are used less in mice and humans, and by increasing the frequencies of those commonly used in these organisms (Figure S1). The codon adaptation index (CAI) was calculated using the codon usage of both humans and mice. The C-G content along the sequences was also adjusted. The synthetic genes were cloned into the pcDNA3 plasmid (Invitrogen), flanked by the *EcoRV* and *XhoI* restriction enzyme sites, generating the pEotmD2 (80% of the *e* gene) and pNS1otmD2 (*ns1* gene) constructs. *Escherichia coli*, DH5- $\alpha$  strain, were subjected to transformation with the recombinant plasmids. To identify positive clones, restriction mapping was performed, and confirmed by sequencing (ABI PRISM dye terminator, Applied Biosystems), carried out by the DNA Sequencing Genomic Platform (Fiocruz, Rio de Janeiro, Brazil).

### 2.4. DNA Vaccine Purification

Production of plasmids was obtained from transformed *E. coli*. Purification of DNA vaccines and the control pcTPA were carried out by alkaline lysis and subsequent purification on ion exchange columns, utilizing the "Qiagen EndoFree Plasmid Mega Kit" (QIAGEN), following the manufacturer's guidelines. Plasmids were suspended in water and stored at -20°C until use. DNA quantification was performed using a Bio Photometer (Eppendorf) at 260 nm.

### 2.5. Cell Transfection and Immunofluorescence Assay

The Neuro2A or Huh7 cells were seeded at a concentration of  $2 \times 10^4$  cells/well in chamber slides (LabTek, Nunc) with Opti-MEM medium (Invitrogen) and cultured overnight at 37 °C with 5% CO<sub>2</sub>. After 24h, cells were transfected with one of the plasmids (pEotmD2, pE1D2, pNS1otmD2, pcTPANS1 or the control pcTPA), using Lipofectamine 2000 (Invitrogen), following the manufacturer's recommendations. For Neuro2A, 0.8  $\mu$ g of the recombinant plasmids were employed, whereas 1.0  $\mu$ g was used for HuH7 cells. The next day, cells were fixed (4% paraformaldehyde in 0.1 M phosphate



buffer, PB), then permeabilized (0.6% saponin in PB) and blocked (1% bovine serum albumin, BSA) (Sigma) and 0.2% saponin in PB). Cells were initially incubated for 1 h at 37 °C with the specified primary antibodies: monoclonal anti-DENV2 3H5 antibody (ATCC), which targets domain III of the E protein, or DENV-2 hyperimmune ascitic fluid (ATCC) that recognizes the NS1 protein. Cells were subsequently incubated for an additional hour at 37 °C with anti-mouse IgG conjugated to FITC (Southern Biotech). The visualization of cells was carried out using the Nikon Eclipse 50i fluorescence microscope (Nikon Inc).

## 2.6. Cell Transfection and Flow Cytometry

The Neuro2A ( $1 \times 10^6$  cells/flask) and HuH7 ( $5 \times 10^5$  cells/flask) were seeded in 75 cm<sup>2</sup> culture flasks, with Opti-MEM medium and cultured overnight at 37 °C with 5% CO<sub>2</sub>. The following day, Neuro2A and HuH7 cells were transfected with 8 µg or 10 µg, respectively, of one of the recombinant plasmids (pEotmD2, pE1D2, pNS1otmD2, pcTPANS1 or pcTPA) using lipofectamine 2000, following the instructions of manufacture. Following a 24-hour incubation, cells were detached using Trypsin-EDTA, fixed (4% paraformaldehyde in PB) and permeabilized (0.05% saponin in PB). For the intracellular staining of E and NS1 proteins, the same antibodies described for the immunofluorescence were used. Ten to twenty thousand events were acquired in a FACS Calibur flow cytometer (BD Bioscience) at the Flow Cytometry Platform of Oswaldo Cruz Institute (IOC-Fiocruz, Rio de Janeiro, Brazil) and data were analyzed using FlowJo v10 (BD Bioscience).

## 2.7. Mice Immunization and Challenge with DENV2

Experiments involving mice were conducted in compliance with ethical principles in animal experimentation outlined by the Brazilian College of Animal Experimentation and approved by the Animal Use Ethical Committee of Oswaldo Cruz Institute, Oswaldo Cruz Foundation (CEUA-IOC approval ID: L039/2015 and L022/2019). Two independent experiments were performed (5 or 10 mice per group). BALB/c mice (specific pathogens free, SPF), male, four-week-old, were acquired from the Multidisciplinary Center for Biological Investigations (CEMIB, UNICAMP, Campinas, SP, Brazil).

Animals received two doses of one of the plasmids via the intramuscular (i.m.) route: pEotmD2, pE1D2, pNS1otmD2, pcTPANS1 or pcTPA. Doses of 100 µg of DNA diluted in 100 µl of phosphate buffer saline (PBS) were administered (50 µg of DNA in each tibialis posterior muscle), two weeks apart. For evaluation of the humoral and cellular immune responses, blood and spleen were collected two weeks after the second DNA dose. Blood samples were obtained by heart puncture. Before receiving the first DNA dose, pre-immune sera were collected from the animals through retro-orbital puncture.

For protection assessment, two weeks after the last DNA vaccine dose, other animal groups were subject to an intracerebral (i.c.) challenge using 30 µL of a neuroadapted NGC DENV2 ( $3.5 \log_{10}$  PFU/mL) diluted in serum-free E199 medium, which corresponds to approximately 40 LD<sub>50</sub>. Non-immunized animals were inoculated with DENV2, serving as a control group. Following the DENV2 challenge, animals were observed for a period of 3 weeks to assess mortality and morbidity. Morbidity was quantified using a subjective scale ranging from 0 to 4: 0 - no clinical signs; 1 - one limb paralysis or spinal column alteration; 2 - severe paralysis in one limb and spinal column alteration or substantial paralysis on both hind limbs; 3 - substantial paralysis in the two hind limbs and spinal column alteration; and 4 - death. Animals were euthanized 21 days after the challenge.

## 2.8. Detection of Antibodies Against the E and NS1 Proteins

The ELISA assay was used to quantify specific anti-E or anti-NS1 antibody titers generated in BALB/c mice after immunization. Two independent experiments were performed with 5 animals per group. For detection of E-specific antibodies in ELISA plates, the solid-phase bound antigen was the domain III of the E protein (EDIII), which was produced in *E. coli* and gently provided by Dr. Luis C. Ferreira (University of São Paulo, SP, Brazil). Anti-NS1 antibodies were detected by using the recombinant NS1 protein (expressed in S2 cells), which was kindly given by Dr. Beth-Ann Collier

(Merck Sharp and Dohme Corp.). The antigens EDIII or NS1 were adsorbed on ELISA MaxiSorp plates (Nunc), at the concentration of 0.2 µg and 0.1 µg for well, respectively, at 37 °C for 1 h. Subsequently, the plates were incubated with a blocking buffer (2% skim milk in 0.05% Tween-20-PBS - PBST), overnight at 4°C. The following day, the plates were washed with PBST and serum samples were added in duplicates with serial dilutions, followed by 1 h incubation at 37 °C. After another round of washing, the plates were incubated with goat anti-mouse IgG conjugated to horseradish peroxidase (Southern Biotechnology) at 37 °C. After 1 hour, plates were washed and reactions were measured at A<sub>490nm</sub> in a microplate reader (SpectraMax 190, Molecular Devices) with OPD (ortho-phenylenediamine dihydrochloride, Sigma) and H<sub>2</sub>O<sub>2</sub>. The reaction was stopped with 9N H<sub>2</sub>SO<sub>4</sub>. The specific antibody titers were calculated as the reciprocal of serum dilution that produced an absorbance above that of the corresponding preimmune serum.

### 2.9. Plaque Reduction Neutralization Test (PRNT50)

Vero cells were seeded overnight in 96-well plates, 2 × 10<sup>4</sup> cells per well, in E199 medium with 5% FBS and cultured at 37 °C with 5% CO<sub>2</sub>. The next day, serum samples were initially subjected to a 56 °C heat treatment for 30 min to inactivate the complement system. Sera were two-fold serially diluted (ranging from 1:20 to 1:1260) in 60 µL of E199 medium. Subsequently, they were mixed with 60 µL of the DENV2 44/2, which contained approximately 30 PFU, and incubated at 37 °C with 5% CO<sub>2</sub>. After 1 hour, 100 µL of the serum/virus mixture were added to Vero cell monolayers in duplicates, and plates were incubated for 1 h at 37 °C with 5% CO<sub>2</sub>. The supernatant of the wells was removed, and 150 µL of E199 medium containing 5% FBS and 2% carboxymethylcellulose (Sigma) were added, and cell monolayers were incubated at 37 °C with 5% CO<sub>2</sub> for five days. The cells were fixed with 10% formalin solution and stained with 0.02% crystal violet for 30 min. Two independent experiments were performed with 5 animals per group. Neutralizing antibody titers were quantified based on a 50% plaque reduction (PRNT50).

### 2.10. Interferon Gamma ELISPOT Assay

The IFN-γ ELISPOT assay was carried out using the IFN-γ ELISPOT mouse set from BD Biosciences in accordance with the manufacturer's instructions. Animals were euthanized two weeks after the second DNA vaccine dose. Splenocytes were isolated and stimulated with synthetic peptides, specific to the CD8<sup>+</sup> T cell, found in the envelope <sup>331</sup>SPCKIPFEI<sup>339</sup> or NS1 <sup>65</sup>AGPWHLGKL<sup>273</sup> proteins [46,47]. In summary, 96-well ELISPOT plates were coated with anti-IFN-γ capture monoclonal antibody (100 µL/well, diluted in PBS), and incubated overnight at 4 °C. The next day, plates were washed with PBS, blocked with RPMI-1640 medium (Sigma) containing 10% FBS for 2 h at 37 °C and splenocytes were seeded in triplicates (5 × 10<sup>5</sup> cells/well) in RPMI-1640 medium with 10% FBS. Non-stimulated and concanavalin A (Con A, 2 µg/well) stimulated cells were used as negative and positive controls, respectively. After 18 hours of incubation at 37 °C with 5% CO<sub>2</sub>, cells were removed, plates were washed with distilled water and PBST, and anti-IFN-γ biotinylated detection antibody was added and incubated for 2 h at 37 °C. Following another round of washing with PBST, the plates were incubated with streptavidin-horseradish peroxidase (HRP) conjugate for 1 hour. Finally, plates were washed with PBST and the spots were revealed by adding the AEC substrate set (BD/Pharmingen) along with hydrogen peroxide (Sigma) for 20 min at room temperature. The reaction was stopped with distilled water and the spots were quantified using an automated immunospot reader (Cellular Technology Ltd.) at the ELISPOT Multi-User Platform (Fiocruz, RJ, Brazil). Two independent experiments were performed with 5 animals per group.

### 2.11. Statistical Analysis

All statistical analysis was conducted using GraphPad Prism v9.0 (GraphPad Software), with a minimum level of significance of 95%. Differences among groups were analyzed by the Kruskal-Wallis test with Dunn's correction for the ELISA, PRNT and ELISPOT experiments. Survival and

morbidity rates were estimated using the Log-Rank (Mantel-Cox) statistical test. Data were displayed as mean  $\pm$  SD and the significance level for each analysis is indicated in the Figure legends.

### 3. Results

#### 3.1. The Effect of Codon Optimization on E and NS1 Protein Expression in Mouse and Human Cells

In this study, we investigated the efficacy of the new DNA vaccines based on E and NS1 dengue proteins. In an attempt to increase antigen expression, we designed synthetic coding sequences for E and NS1 DENV2 proteins based on codons frequently used in both mouse and human cells. The codon optimization process increased the CAI from 0.71 to 0.87 for the envelope sequence and from 0.74 to 0.87 for the *ns1* gene. In the optimized sequences, the CG content was also changed from 45.08% to 52.34% in envelope and from 44.79% to 51.17% in *ns1* sequences. Peaks of %GC content in a 60 bp window were eliminated.

The codon optimized DNA vaccines were referred to as pEotmD2 and pNS1otmD2, while the previous constructs encoding the native *e* and *ns1* genes were named pE1D2 and pcTPANS1, respectively. The antigen expression was evaluated *in vitro* by immunofluorescence and flow cytometry after the transfection of mouse Neuro2A and human HuH7 cells. The percentage of Envelope- or NS1-positive cells and the mean fluorescence intensity (MFI) were compared between the original (pE1D2 and pcTPANS1) and the codon-optimized plasmids (pEotmD2 and pcTPANS1). Flow cytometry gating strategy is represented in Figure S2.

The E protein was detected in both Neuro2A (Figure 1A), and HuH7 (Figure 1B) cells transfected either with pE1D2 or pEotmD2, showing that the new codon-optimized pEotmD2 construct retained its ability to mediate antigenic expression. We observed more E-positive Neuro2a cells when transfected with the plasmid pE1D2 compared to pEotmD2. This difference was also reflected in HuH7 cells, but to a lesser extent (Figure 1C). Regarding the envelope expression, differences between transfections were only detected in HuH7 cells, in which the pE1D2 plasmid led to higher protein production when compared to the codon optimized DNA pEotmD2 (Figure 1D).

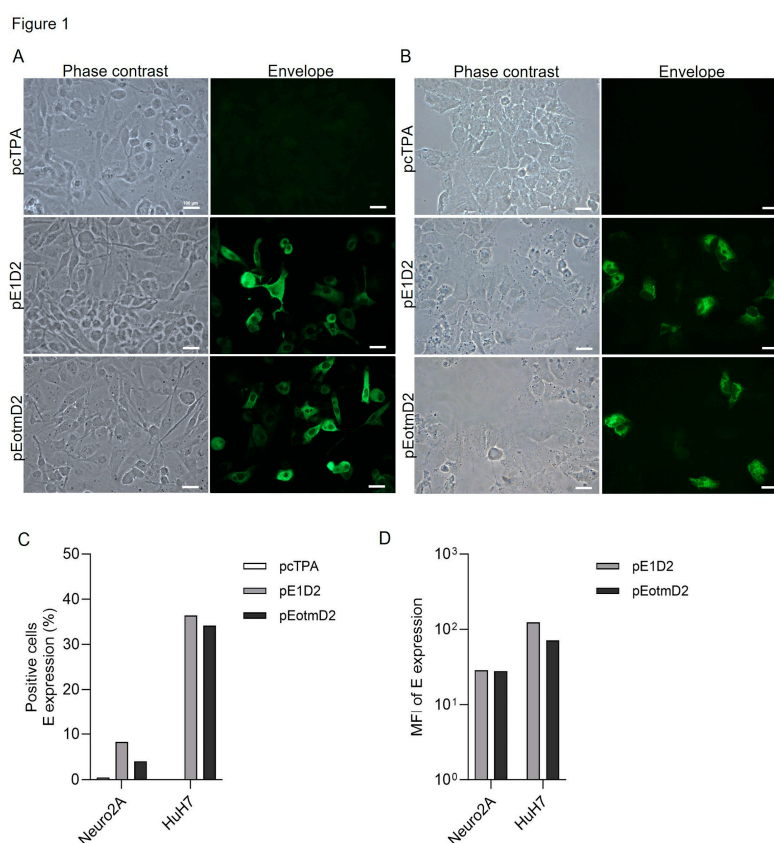


**Figure 1.** In vitro expression of the envelope protein in transfected cells. Immunofluorescence and flow cytometry of Neuro2A and HuH7 cells transiently transfected with pE1D2 or pEotmD2 plasmids, or with negative control pcTPA. After the 24h-transfection, the E protein was detected with the mouse 3H5 monoclonal antibody (anti-EDIII) followed by Alexa Fluor 488-conjugated goat anti-mouse IgG antibody (A–D). Phase contrast and immunofluorescence images of Neuro2A (A) and HuH7 (B) transfected cells. Images were acquired in the Nikon H550S fluorescence microscope at 40X (Scale white bar, 100  $\mu$ m). Frequencies (C) and mean of fluorescence intensity (D) of E-positive Neuro2A and HuH7 cells were quantified by flow cytometry.

The NS1 expression seemed to be slightly more effective when mediated by the codon optimized pNS1otmD2 plasmid. The protein was detected in Neuro2a (Figure 2A) and HuH7 (Figure 2B) transfected with both DNAs, pcTPANS1 and pNS1otmD2. In Neuro2A cells, the percentage of NS1-positive cells were somewhat higher when transfected with the pNS1otmD2 than with the pcTPANS1 (Figure 2C). This difference was more accentuated in human HuH7 cells (Figure 2C). However, levels of the NS1 expressed in the two cell lines were similar, as evidenced by the MFI (Figure 2D). As anticipated, cells transfected with the control pcTPA plasmid showed no positivity for the E or NS1 detection (Figures 1 and 2).

Figure 2

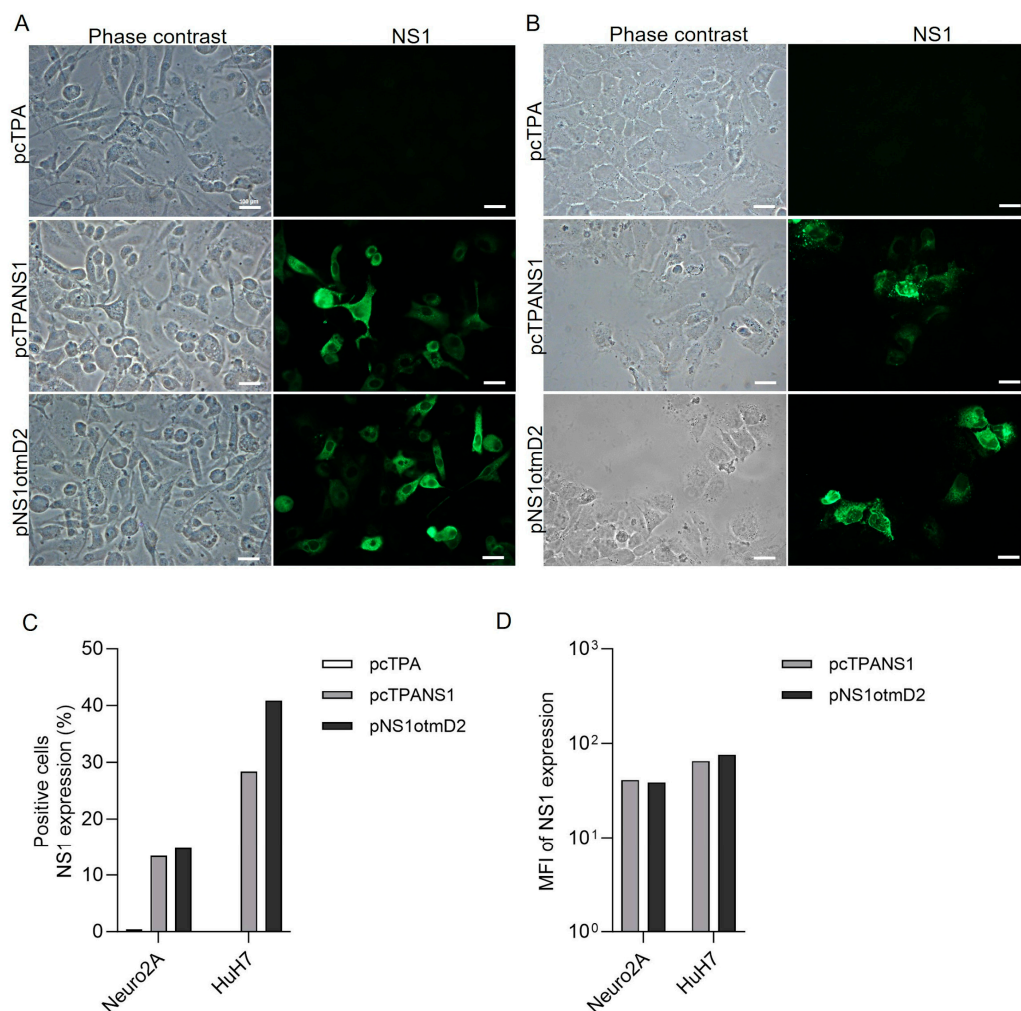


**Figure 2.** In vitro expression of the NS1 protein in transfected cells. Immunofluorescence and flow cytometry of Neuro2A and HuH7 cells transiently transfected with the pcTPANS1 or pNS1otmD2 plasmids, or with negative control pcTPA. After the 24h-transfection, the NS1 protein was detected with the DENV-2 hyperimmune mouse ascitic fluid followed by Alexa Fluor 488-conjugated goat anti-rabbit IgG antibody (A–D). Phase contrast and immunofluorescence images of Neuro2A (A) and



HuH7 (B) transfected cells. Images were acquired in the Nikon H550S fluorescence microscope at 40X (Scale white bar, 100  $\mu$ m). Frequencies (C) and mean of fluorescence intensity (D) of NS1-positive Neuro2A and HuH7 cells were quantified by flow cytometry.

### 3.2. The Humoral and Cellular Immune Responses Generated by Optimized or Original DNA vaccines

The effect of codon optimization on the immunogenicity of the DNA vaccines encoding the E or NS1 proteins was evaluated in immunized BALB/c mice. Two weeks after full vaccination, mouse sera and splenocytes were collected for assessment of antibody and T-cell responses (Figure 3A).

Figure 3

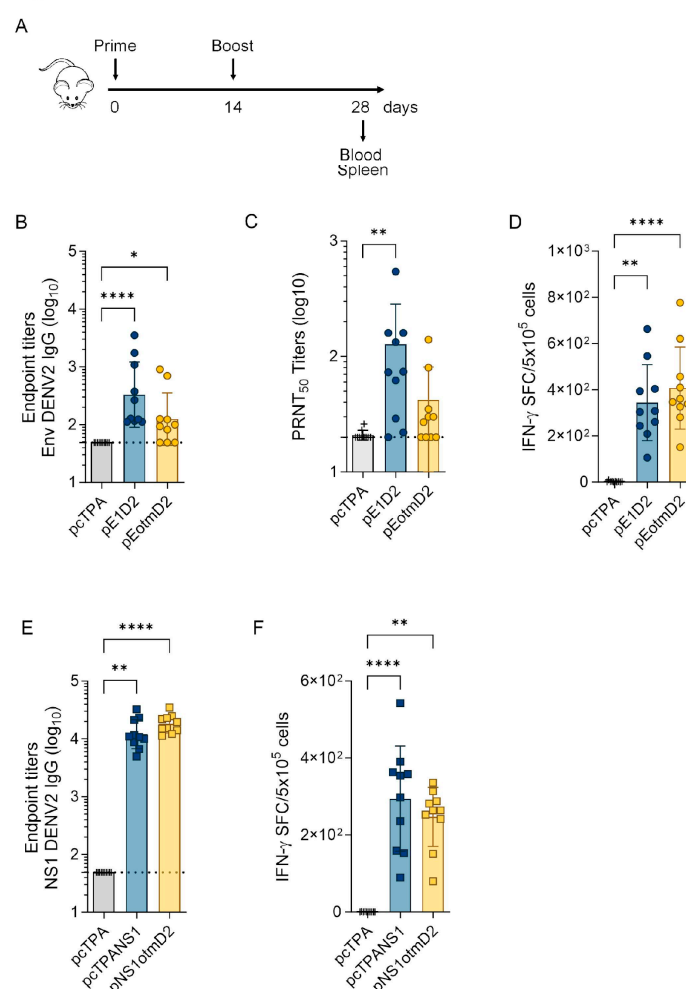


**Figure 3.** Immunogenicity of the DNA vaccines in mice. BALB/c mice were i.m. immunized with two doses of the different plasmids. Blood and spleens were harvested 14 days post-immunization to analyze the antibody and T cell responses (A). ELISA, using EDIII (B) or NS1 (E) proteins, and PRNT50 (C) were performed with serum samples from mice immunized with the different DNA vaccines or with the negative control pcTPA. Serum samples were individually tested in duplicates and bars represent the mean of the obtained values (B, C and E). IFN- $\gamma$  production by ELISPOT assays were performed by stimulating splenocytes with the synthetic E<sup>331</sup>SPCKIPFEI<sup>339</sup> (D) or NS1<sup>265</sup>AGPWHLGKL<sup>273</sup> (F) peptides. Splenocytes were individually stimulated in triplicates and the bars represent the group's mean values (D,F). Statistical differences between groups were calculated using non-parametric Kruskal-Wallis test (\*p<0.05; \*\*p<0.01; \*\*\*\*p<0.0001). (B-F) Data are representative of two independent experiments (n=10).

Regarding the E protein, we detected significant EDIII-specific antibody titers in animals immunized either with pE1D2 or pEotmD2, although the magnitude of this response was lower in

the group inoculated with the optimized DNA when compared to mice vaccinated with the original plasmid, pE1D2 (Figure 3B). These results were also reflected in serum neutralization assays. The DENV2 neutralizing antibody titers in mice immunized with the pE1D2-DNA vaccine were statistically different compared to the pcTPA control group (Figure 3C). Mice vaccinated with the pEotmD2 also showed detectable neutralizing antibodies, although titers were lower when compared to the pE1D2-inoculated animals and not statistically different from the control group (Figure 3C).

Concerning the cellular immune response, we observed significant IFN- $\gamma$  production by T-cells collected from animals vaccinated either with the pE1D2 or the pEotmD2 plasmid. Furthermore, unlike the antibody response, the pEotmD2-immunized group showed a slightly higher number of E-specific T-cells than pE1D2-inoculated mice (Figure 3D).

The pcTPANS1 and pNS1otmD2 DNA vaccines, in turn, induced similar anti-NS1 antibody levels, statistically higher than the control pcTPA group (Figure 3E). Both vaccines also activated specific IFN- $\gamma$ -producing T cell response upon stimulation with the NS1 peptide. Although not statistical, the number of NS1-specific T cells was slightly higher after vaccination with the pcTPANS1 in comparison with the codon-optimized pNS1otmD2 (Figure 3F).

### 3.3. Codon Optimization Failed to Improve the Efficacy the NS1- or E-Based DNA Vaccines

To assess the impact of codon optimization on the protection generated by the DNA vaccines, immunized BALB/c mice were challenged with DENV2, two weeks after full vaccination (Figure 4A). The efficacy of vaccination was assessed daily by survival and morbidity.

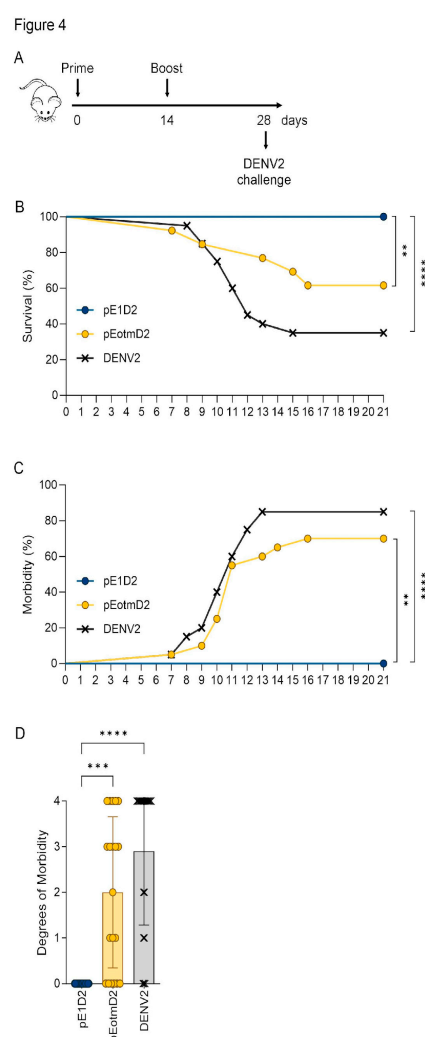


**Figure 4.** Protection in mice immunized with the E-based DNA vaccines after a lethal DENV2 challenge. BALB/c mice were i.m. immunized with two doses of the pE1D2 or pEotmD2 vaccines,

challenged with DENV2 inoculated by the i.c. route two weeks after full vaccination, and monitored for 21 days (A) for assessment of survival (B), morbidity (C) rates, and the different morbidity degrees (D). A semi-quantitative analysis of the clinical signs of infection was made using a morbidity degree scale from 0 to 4. Bars represent the median of the observed degrees (D). Statistical differences between groups were calculated using Log-Rank (Mantel-Cox) (B,C) or non-parametric Kruskal-Wallis tests (D) (\*\*p<0.01; \*\*\*p<0.001; \*\*\*\*p<0.0001). Data are representative of two independent experiments (n=20).

Immunization with the pE1D2 DNA vaccine generated 100% survival against the DENV2 challenge. However, the group immunized with the optimized plasmid pEotmD2 showed 60% survival, with deaths starting on the 7th day after challenge. In contrast, only 35% of non-immunized DENV2-challenged mice survived, with peak death between the 7th and 15th days post-infection (Figure 4B). Morbidity was also observed, regarding the percentage of affected mice as well as according to an arbitrary pre-defined score scale of clinical signs of infection. The pE1D2 DNA vaccine provided full protection against DENV2, since no mice presented any infection sign (Figure 4C,D). Conversely, around 70% of pEotmD2-immunized mice showed morbidity (Figure 4C), with a high number of animals reaching the 3 or 4 morbidity degrees (Figure 4D). As expected, most non-immunized mice (85%) showed clinical signs of infection (Figure 4C,D). Furthermore, no statistical differences were observed between the pEotmD2 and non-immunized groups concerning the survival or morbidity parameters, thus indicating that codon optimization impaired protection generated by the E-based DNA vaccine.

The pcTPANS1 and the codon-optimized pNS1otmD2 generated high percentages of protection, with 90% and 100%, survival rates, respectively (Figure 5A). Only 10% of the pcTPANS1-immunized mouse group showed the highest degree of morbidity between days 7 and 10 post-infection (Figure 5B,C). Although all pNS1otmD2-vaccinated animals survived virus challenge, 15% of them showed morbidity between the 13th and 15th days post-infection (Figure 5D) with degrees varying between 1, and 3 (Figure 5C). Thus, the two NS1 DNA vaccines generated significant protection compared to the non-immunized group, either in terms of survival or morbidity (Figure 5). Although there were no statistical differences between groups immunized with the pcTPANS1 compared to the codon-optimized pNS1otmD2 plasmid, the 100% survival rate from the pNS1otmD2 group reveals a slight improvement in vaccination-mediated protection.

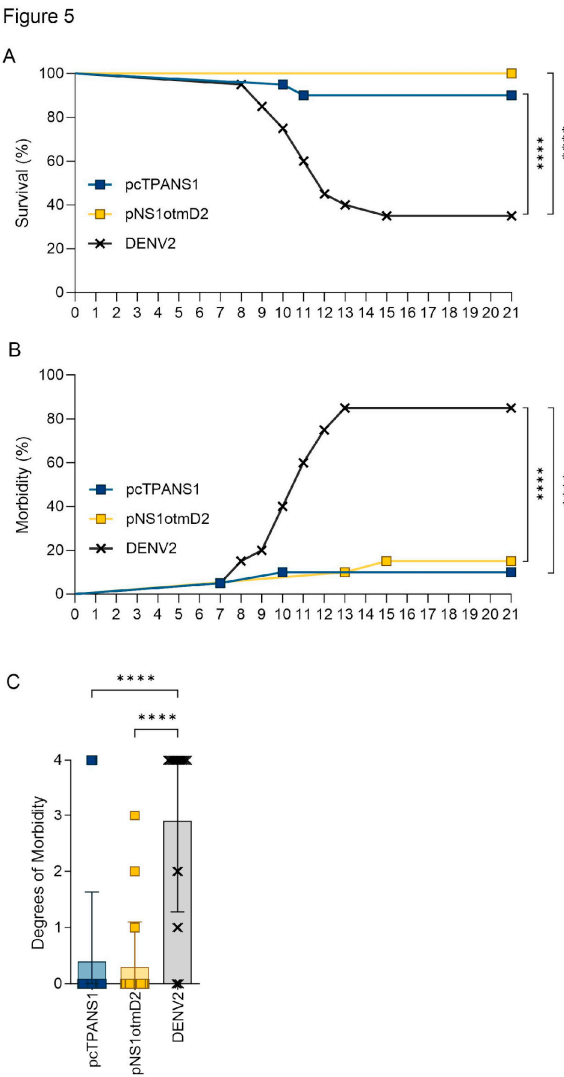


**Figure 5.** Protection in mice immunized with the NS1-based DNA vaccines after a lethal DENV2 challenge. BALB/c mice were immunized with the pcTPANS1 and pNS1otmD2 vaccines, challenged with DENV2 and monitored (as described in fig 4) for 21 days for assessment of survival (A), morbidity (B) rates, and the different morbidity degrees (C). A semi-quantitative analysis of the clinical signs of infection was made using a morbidity degree scale from 0 to 4, as described in fig 4. Bars represent the median of the observed degrees (C). Statistical differences between groups were calculated using Log-Rank (Mantel-Cox) (A,B) or non-parametric Kruskal–Wallis tests (C) (\*\*\*p<0.0001). Data are representative of two independent experiments (n=20).

4. Discussion

Considerable efforts have been made to improve the immunogenicity and efficacy of the dengue DNA vaccine, such as exploring alternative administration routes, employing immunostimulatory CpG motifs, optimizing codons, incorporating genetic adjuvants, and implementing heterologous prime/boost regimens [10,21,48].

Within this context, in previous studies our group assessed a range of DNA vaccine constructs focused on the DENV2 E and NS1 antigens. The objective was to identify the most effective design for eliciting robust immunogenicity and providing protection. Four DENV2 NS1 DNA vaccines were developed, each with unique designs. Two constructs, pcTPANS1ANC and pcENS1ANC, utilized a hydrophobic segment from NS2a to direct NS1 to cell surfaces, while the other two, pcTPANS1 and pcENS1, were designed for protein secretion. These differences affected NS1 expression in mammalian cells, and consequently the resulting immunogenicity and protection *in vivo*. Among these different



DNA vaccines, the pcTPANS1 and pcENS1 triggered the most robust antibody responses and protection, with the pcTPANS1 eliciting a slightly superior level of protection [34]. Regarding the envelope protein, two vaccines were constructed: the pE1D2, containing the ectodomain (DI, DII and DIII) of the DENV2 E sequence and the pE2D2, containing only the DIII sequence, both fused to t-PA sequence. Both vaccines elicited neutralizing antibodies, but pE1D2 provided greater protection compared to pE2D2 [44]. Additionally, pcTPANS1 and pE1D2 were effective in inducing a cellular immune response in mice [49].

Therefore, given the protective efficacy of these two vaccines, in the present investigation, the nucleotide sequences encoding the envelope ectodomain and NS1 proteins were codon-optimized for expression in both murine and human cells. The objective of this work was to further increase the protective capacity of these DNA vaccines either in murine experimental models or in future clinical trials. Codon optimization is an important approach for enhancing protein expression in heterologous systems, such as DNA vaccines. Such approach, which exploits the degenerate nature of the genetic code, alters several critical parameters for expression efficiency, such as codon usage bias, GC content, mRNA secondary structure, cryptic splicing sites, premature PolyA sites, among others [50–52]. Several studies have evidenced that codon optimization leads to an increase not only in protein expression, but also in the immunogenicity and protection of several DNA vaccines for different pathogens [53–59].

Initially, *in vitro* tests were carried out to compare the ability of the plasmids containing the native genes, pE1D2 and pcTPANS1, with the codon-optimized constructs, pEotmD2 and pcNS1otmD2, in mediating E and NS1 proteins expression in both murine and human cell lines. Assessment of transfection efficiency revealed that the optimized pEotmD2 plasmid exhibited slightly lower performance compared to the pE1D2, while the codon-optimized plasmid pcNS1otmD2 demonstrated slightly superior efficiency in comparison to the pcTPANS1.

Analysis of the humoral immune response generated by plasmids encoding the E protein aligns with the lower protein production observed *in vitro*. Overall, immunization with the original pE1D2 plasmid elicited slightly higher levels of E-specific and neutralizing antibodies compared to immunization with the pEotmD2, though these differences were not statistical. In contrast, alteration in the E protein codons had an inverse effect on the cellular immune response, in which the pEotmD2 was slightly more effective in stimulating the IFN- $\gamma$  production. The protection evaluation against a neuroadapted DENV2 showed that immunization with the pE1D2 was statistically more effective when compared to the pEotmD2. Indeed, the pE1D2 exhibited robust protection, consistent with earlier observations [44,60,61]. In contrast, protection conferred by the plasmid harboring the optimized gene, pEotmD2, was relatively modest and did not exhibit statistical differentiation from the control group. Thus, although no major difference was observed in the envelope expression level nor in the humoral immune response, the codon changes of the E protein substantially affected the protective capacity of the DNA vaccine.

Concerning the plasmids encoding the NS1 protein, administration of the pcNS1otmD2 induced marginally higher antibody levels than the pcTPANS1-immunized group. Similarly, the pcNS1otmD2 provided slightly superior levels of protection compared to the pcTPANS1, yet without significant statistical differences. The analysis of the humoral immune response and protection correlates with the findings of *in vitro* experiments, in which the pcNS1otmD2 plasmid demonstrated greater efficiency compared to the pcTPANS1. Considering that optimization efficiency can be influenced by the host system and given that the enhancement in the *in vitro* NS1 expression mediated by pcNS1otmD2 was higher in human than in murine cells, there is a possibility that this codon-optimized vaccine could induce a more robust protective response in primate models or in humans.

Overall, codon optimization is a useful strategy for the designing of DNA vaccines, but it does not guarantee an increase in recombinant protein expression or in the protective immunity induced by the vaccine [62]. In the present investigation, although the codon optimization of E and NS1 sequences for human and mouse cells did lead to an increase in the CAI and an adjustment in GC content, this process had divergent effects on the expression of these two proteins and on the immunogenicity and protective capabilities of the two vaccines. Surprisingly, the envelope sequence

optimization yielded an opposite effect to what was expected, with a decrease in its performance regarding the expression of the recombinant protein and the induced immunity. Although it is not possible to establish a direct correlation, the reduced efficacy of pEotmD2 in the *in vivo* experiments probably reflects the lower efficiency of this plasmid in mediating the envelope protein *in vivo* expression. Interestingly, the pEotmD2 plasmid elicited slightly higher levels of cellular response than the pE1D2 plasmid.

Other research groups also observed a reduction in the recombinant protein production by employing a codon optimization strategy. The sequence modification of the gene that codes a human potassium channel (hERG) by employing synonymous codon substitutions to adjust GC content, reduced the incidence of rare codons and minimize mRNA secondary structure, resulting in protein expression decreased in HEK293T cells [63,64]. Agashe et al. [65] observed that creation of synonymous variants for a critical gene coding an enzyme in *Methylobacterium extorquens* resulted in substantially reduced gene expression and enzymatic activity compared to the wild-type version. Notably, using solely rare codons in the gene led to a 40% decrease in fitness, while a sequence entirely comprised of frequent codons caused a more dramatic reduction in fitness, exceeding 90%.

Synonymous modifications in the coding region can influence both mRNA stability and protein properties, including conformation, stability, post-translational modification sites, and even its functionality [51,62,64]. One possible explanation for the reduced efficiency of pEotmD2 in comparison to pE1D2 could be attributed to codon substitutions influencing protein folding. Thus, even if the amino acid sequence remains unchanged, variations in the translation speed may result in the generation of distinct protein structures. Such structural variances could influence E epitopes and, as a result, impact the quality and protective potential of the immune response elicited against this protein. Alterations in the E protein folding may also have increased its transportation for processing and subsequent presentation to T cells. Several reports have demonstrated the influence of synonymous codon substitution on the folding of the recombinant protein [66–70]. Hu and colleagues [69] studied the effects of synonymous codons on the properties of the anti-human IgE antibody produced in *Escherichia coli*. Authors generated 342 codon variants and observed that expression of the recombinant protein in bacteria resulted in antibodies that differed significantly in solubility and functionality, with antigen-binding activity ranging from no binding to a high binding affinity. The circular dichroism (CD) analysis of enhanced-affinity variants revealed noticeable structural and conformational alterations. In another study focused on the fluorescent protein YKB (yellow-black-blue), authors examined whether altering synonymous codons could result in variations in its conformation and, consequently, its fluorescent properties. The findings of this investigation underscored that even minor changes in codon usage can result in significant alterations in protein folding [68]. In a report on *Neurospora* cell-free translation system, it was noted that, despite a codon-optimized luciferase mRNA completing translation elongation more quickly than the wild-type mRNA and yielding a greater quantity of protein, a substantial portion of the protein turned out to be non-functional. These results indicated that codon usage affects translation elongation speed, consequently impacting on protein functionality by regulating co-translational folding [70].

The impact of codon optimization is subject to variation depending on the specific antigen, pathogen, and host system chosen. In most studies, the increased expression of recombinant proteins mediated by codon-optimized DNA vaccines correlates with enhanced immune responses and superior protection when compared to vaccines containing native genes [54–59]. Nevertheless, some reports have shown that the increase in expression mediated by plasmids containing codon-optimized genes does not consistently result in enhanced immunogenicity or increased protection [71–73]. In the evaluation of a DNA vaccine based on FimH, a protein involved in the adhesion of uropathogenic *Escherichia coli* (UPEC) to epithelial cells, authors observed that, although the DNA vaccine containing mammalian codon-optimized fimH gene exhibited higher expression levels compared to the DNA vaccine with native gene, both vaccines were equally effective in conferring protection in mice, with no significant difference between them [73]. In another study, the impact of mammalian codon optimization on the immunogenicity and protective potential of DNA vaccines

encoding antigens from the pre-erythrocytic stage of *Plasmodium falciparum* and *Plasmodium yoelii* was assessed in mice. While codon optimization notably enhanced *in vitro* antigen expression, it did not lead to an improvement in antigen-specific T-cell responses or protection. [72]. Döşkaya and colleagues [71], in their analysis of a codon-optimized DNA vaccine against *T. gondii*, observed that the immune response and protective efficacy of the codon-optimized GRA1 DNA vaccine were slightly superior to those of the wild-type GRA1 DNA vaccine. These results resemble those observed in *in vivo* assessments of the pNS1otmD2 plasmid, which yielded slightly greater protection levels than the pcTPANS1.

Our study revealed contrasting results for codon optimization of the two dengue DNA vaccines. While the vaccine encoding the envelope protein demonstrated reduced efficacy, the vaccine containing the ns1 gene exhibited slightly enhanced protection in the murine model. An important consideration in our study is that codon optimization was targeted to two systems: mouse cells and human cells. This adaptation may have affected the optimal protein expression pattern in each of these systems and, consequently, influenced the observed results.

The outcome of codon optimization may differ in each unique case, and accurately predicting the impact of synonymous codon usage on the properties of an antigen or the immunogenicity of a vaccine is a challenge. Hence, although codon optimization is a highly valuable tool in the development of DNA vaccines, its application demands thorough evaluation.

**Supplementary Materials:** The following supporting information can be downloaded at the website of this paper posted on Preprints.org.

**Author Contributions:** Conceptualization, A.M.B.A. and S.M.C.; methodology, S.M.C., A.R.P., P.B.A.P., M.L.A., P.R., R.L.C.S. and M.M.B.; formal analysis, A.M.B.A., S.M.C., A.R.P. and P.B.A.P.; investigation, A.M.B.A., S.M.C., A.R.P. and P.B.A.P.; resources, A.M.B.A.; writing—original draft preparation, S.M.C., A.R.P., P.B.A.P. and A.M.B.A.; writing—review and editing, S.M.C. and A.M.B.A.; supervision, A.M.B.A.; project administration, A.M.B.A.; funding acquisition, A.M.B.A. All authors have read and agreed to the published version of the manuscript.

**Funding:** The work was funded by the Brazilian National Research Council (CNPq) (grant number: 302639/2022-5), the Carlos Chagas Filho Foundation for Research Support of the State of Rio de Janeiro (FAPERJ) (grant number E- 26/010.001959/2019), the National Institute of Science and Technology in Vaccines (INCTV) (grant number 573547/2013), the Coordination of Improvement of Higher Education Personnel (CAPES) (grant number 88887.694977/2022-00), and the Oswaldo Cruz Institute (grand number IOC-008-FIO-22-2-23).

**Institutional Review Board Statement:** The study was conducted in accordance with the ethical principles in animal experimentation stated in the Brazilian College of Animal Experimentation and approved by the Animal Use Ethical Committee of Oswaldo Cruz Institute in Oswaldo Cruz Foundation (CEUA-IOC approval ID: L039/2015 and L022/2019).

**Informed Consent Statement:** Not applicable.

**Data Availability Statement:** Data are available upon reasonable request to the corresponding author.

**Acknowledgments:** We are greatly in debt to Luis Carlos S. Ferreira (Laboratory of Vaccine Development, Department of Microbiology, USP, Brazil) and Beth-Ann Collier (Merck Sharp and Dohme Corp., West Point, PA, USA) for kindly supplying the recombinant EDIII and NS1 proteins, respectively, used in ELISA assays. We would like to thank the Multi-user Research Facility of Flow Cytometry of Instituto Oswaldo Cruz, Fiocruz-RJ, the ELISPOT Platform and the Genomic Platform-DNA Sequencing of Fiocruz-RJ for their technical assistance. We also thank the Center of Animal Experimentation of the Oswaldo Cruz Institute (CEA/IOC).

**Conflicts of Interest:** The authors declare no conflict of interest. The funders had no role in the design of the study; in the collection, analyses, or interpretation of data; in the writing of the manuscript; or in the decision to publish the results”.

## References

1. Brady, O.J.; Gething, P.W.; Bhatt, S.; Messina, J.P.; Brownstein, J.S.; Hoen, A.G.; Moyes, C.L.; Farlow, A.W.; Scott, T.W.; Hay, S.I. Refining the Global Spatial Limits of Dengue Virus Transmission by Evidence-Based Consensus. *PLoS Negl Trop Dis* **2012**, *6*, e1760. <https://doi.org/10.1371/journal.pntd.0001760>.
2. Organization, W.H. Ending the Neglect to Attain the Sustainable Development Goals: A Road Map for Neglected Tropical Diseases 2021–2030: Overview; World Health Organization, 2020; ISBN 978-92-4-001879-2.

3. Wilder-Smith, A.; Ooi, E.-E.; Horstick, O.; Wills, B. Dengue. *The Lancet* **2019**, *393*, 350–363. [https://doi.org/10.1016/S0140-6736\(18\)32560-1](https://doi.org/10.1016/S0140-6736(18)32560-1).
4. Apte-Sengupta, S.; Sirohi, D.; Kuhn, R.J. Coupling of Replication and Assembly in Flaviviruses. *Current Opinion in Virology* **2014**, *9*, 134–142. <https://doi.org/10.1016/j.coviro.2014.09.020>.
5. Tayal, A.; Kabra, S.K.; Lodha, R. Management of Dengue: An Updated Review. *Indian J Pediatr* **2023**, *90*, 168–177. <https://doi.org/10.1007/s12098-022-04394-8>.
6. Guzman, M.G.; Alvarez, M.; Halstead, S.B. Secondary Infection as a Risk Factor for Dengue Hemorrhagic Fever/Dengue Shock Syndrome: An Historical Perspective and Role of Antibody-Dependent Enhancement of Infection. *Arch Virol* **2013**, *158*, 1445–1459. <https://doi.org/10.1007/s00705-013-1645-3>.
7. Anderson, K.B.; Gibbons, R.V.; Cummings, D.A.T.; Nisalak, A.; Green, S.; Libraty, D.H.; Jarman, R.G.; Srikiatkachorn, A.; Mammen, M.P.; Darunee, B.; et al. A Shorter Time Interval Between First and Second Dengue Infections Is Associated With Protection From Clinical Illness in a School-Based Cohort in Thailand. *The Journal of Infectious Diseases* **2014**, *209*, 360–368. <https://doi.org/10.1093/infdis/jit436>.
8. Katzelnick, L.C.; Gresh, L.; Halloran, M.E.; Mercado, J.C.; Kuan, G.; Gordon, A.; Balmaseda, A.; Harris, E. Antibody-Dependent Enhancement of Severe Dengue Disease in Humans. *Science* **2017**, *358*, 929–932. <https://doi.org/10.1126/science.aan6836>.
9. Wilder-Smith, A. Dengue Vaccine Development by the Year 2020: Challenges and Prospects. *Current Opinion in Virology* **2020**, *43*, 71–78. <https://doi.org/10.1016/j.coviro.2020.09.004>.
10. Huang, C.-H.; Tsai, Y.-T.; Wang, S.-F.; Wang, W.-H.; Chen, Y.-H. Dengue Vaccine: An Update. *Expert Review of Anti-infective Therapy* **2021**, *19*, 1495–1502. <https://doi.org/10.1080/14787210.2021.1949983>.
11. Capeding, M.R.; Tran, N.H.; Hadinegoro, S.R.S.; Ismail, H.I.H.M.; Chotpitayasunondh, T.; Chua, M.N.; Luong, C.Q.; Rusmil, K.; Wirawan, D.N.; Nallusamy, R.; et al. Clinical Efficacy and Safety of a Novel Tetravalent Dengue Vaccine in Healthy Children in Asia: A Phase 3, Randomised, Observer-Masked, Placebo-Controlled Trial. *The Lancet* **2014**, *384*, 1358–1365. [https://doi.org/10.1016/S0140-6736\(14\)61060-6](https://doi.org/10.1016/S0140-6736(14)61060-6).
12. Villar, L.; Dayan, G.H.; Arredondo-García, J.L.; Rivera, D.M.; Cunha, R.; Deseda, C.; Reynales, H.; Costa, M.S.; Morales-Ramírez, J.O.; Carrasquilla, G.; et al. Efficacy of a Tetravalent Dengue Vaccine in Children in Latin America. *N Engl J Med* **2015**, *372*, 113–123. <https://doi.org/10.1056/NEJMoa1411037>.
13. Dengue Vaccines: WHO Position Paper – September 2018 Available online: <https://www.who.int/publications-detail-redirect/who-wer9335-457-476> (accessed on 1 November 2023).
14. Halstead, S.B. Safety Issues from a Phase 3 Clinical Trial of a Live-Attenuated Chimeric Yellow Fever Tetravalent Dengue Vaccine. *Human Vaccines & Immunotherapeutics* **2018**, *14*, 2158–2162. <https://doi.org/10.1080/21645515.2018.1445448>.
15. Huang, C.Y.-H.; Butrapet, S.; Tsuchiya, K.R.; Bhamarapravati, N.; Gubler, D.J.; Kinney, R.M. Dengue 2 PDK-53 Virus as a Chimeric Carrier for Tetravalent Dengue Vaccine Development. *J Virol* **2003**, *77*, 11436–11447. <https://doi.org/10.1128/JVI.77.21.11436-11447.2003>.
16. Rivera, L.; Biswal, S.; Sáez-Llorens, X.; Reynales, H.; López-Medina, E.; Borja-Tabora, C.; Bravo, L.; Sirivichayakul, C.; Kosalaraksa, P.; Martinez Vargas, L.; et al. Three-Year Efficacy and Safety of Takeda's Dengue Vaccine Candidate (TAK-003). *Clinical Infectious Diseases* **2022**, *75*, 107–117. <https://doi.org/10.1093/cid/ciab864>.
17. Sheridan, C. First COVID-19 DNA Vaccine Approved, Others in Hot Pursuit. *Nat Biotechnol* **2021**, *39*, 1479–1482. <https://doi.org/10.1038/d41587-021-00023-5>.
18. Baghban, R.; Ghasemian, A.; Mahmoodi, S. Nucleic Acid-Based Vaccine Platforms against the Coronavirus Disease 19 (COVID-19). *Arch Microbiol* **2023**, *205*, 150. <https://doi.org/10.1007/s00203-023-03480-5>.
19. Yadav, T.; Kumar, S.; Mishra, G.; Saxena, S.K. Tracking the COVID-19 Vaccines: The Global Landscape. *Human Vaccines & Immunotherapeutics* **2023**, *19*, 2191577. <https://doi.org/10.1080/21645515.2023.2191577>.
20. Hobernik, D.; Bros, M. DNA Vaccines—How Far From Clinical Use? *IJMS* **2018**, *19*, 3605. <https://doi.org/10.3390/ijms19113605>.
21. Li, L.; Saade, F.; Petrovsky, N. The Future of Human DNA Vaccines. *Journal of Biotechnology* **2012**, *162*, 171–182. <https://doi.org/10.1016/j.jbiotec.2012.08.012>.
22. Li, Z.; Feng, S.; Zhang, H.; Zhuang, X.; Shang, C.; Sun, S.; Han, J.; Xie, Y.; Zhang, J.; Wang, W.; et al. Immunogenicity and Protective Efficacy of a DNA Vaccine Inducing Optimal Expression of the SARS-CoV-2 S Gene in hACE2 Mice. *Arch Virol* **2022**, *167*, 2519–2528. <https://doi.org/10.1007/s00705-022-05562-z>.
23. Kuhn, R.J.; Zhang, W.; Rossmann, M.G.; Pletnev, S.V.; Lenches, E.; Jones, C.T.; Mukhopadhyay, S.; Strauss, E.G.; Baker, T.S.; Strauss, J.H. Structure of Dengue Virus: Implications for Flavivirus Organization, Maturation, and Fusion. **2014**.
24. Stiasny, K.; Kössl, C.; Lepault, J.; Rey, F.A.; Heinz, F.X. Characterization of a Structural Intermediate of Flavivirus Membrane Fusion. *PLoS Pathog* **2007**, *3*, e20. <https://doi.org/10.1371/journal.ppat.0030020>.
25. Hu, T.; Wu, Z.; Wu, S.; Chen, S.; Cheng, A. The Key Amino Acids of E Protein Involved in Early Flavivirus Infection: Viral Entry. *Virol J* **2021**, *18*, 136. <https://doi.org/10.1186/s12985-021-01611-2>.
26. Modis, Y.; Ogata, S.; Clements, D.; Harrison, S.C. Structure of the Dengue Virus Envelope Protein after Membrane Fusion. *Nature* **2004**, *427*, 313–319. <https://doi.org/10.1038/nature02165>.



27. Modis, Y.; Ogata, S.; Clements, D.; Harrison, S.C. Variable Surface Epitopes in the Crystal Structure of Dengue Virus Type 3 Envelope Glycoprotein. *J Virol* **2005**, *79*, 1223–1231. <https://doi.org/10.1128/JVI.79.2.1223-1231.2005>.
28. Tsai, W.-Y.; Lin, H.-E.; Wang, W.-K. Complexity of Human Antibody Response to Dengue Virus: Implication for Vaccine Development. *Front. Microbiol.* **2017**, *8*, 1372. <https://doi.org/10.3389/fmicb.2017.01372>.
29. Rothman, A.L. Immunity to Dengue Virus: A Tale of Original Antigenic Sin and Tropical Cytokine Storms. *Nat Rev Immunol* **2011**, *11*, 532–543. <https://doi.org/10.1038/nri3014>.
30. Rivino, L. Understanding the Human T Cell Response to Dengue Virus. In *Dengue and Zika: Control and Antiviral Treatment Strategies*; Hilgenfeld, R., Vasudevan, S.G., Eds.; Advances in Experimental Medicine and Biology; Springer Singapore: Singapore, 2018; Vol. 1062, pp. 241–250 ISBN 978-981-10-8726-4.
31. Flamand, M.; Megret, F.; Mathieu, M.; Lepault, J.; Rey, F.A.; Deubel, V. Dengue Virus Type 1 Nonstructural Glycoprotein NS1 Is Secreted from Mammalian Cells as a Soluble Hexamer in a Glycosylation-Dependent Fashion. *J Virol* **1999**, *73*, 6104–6110. <https://doi.org/10.1128/JVI.73.7.6104-6110.1999>.
32. Young, P.R.; Hilditch, P.A.; Bletchly, C.; Halloran, W. An Antigen Capture Enzyme-Linked Immunosorbent Assay Reveals High Levels of the Dengue Virus Protein NS1 in the Sera of Infected Patients. *J Clin Microbiol* **2000**, *38*, 1053–1057. <https://doi.org/10.1128/JCM.38.3.1053-1057.2000>.
33. Avirutnan, P.; Zhang, L.; Punyadee, N.; Manuyakorn, A.; Puttikhunt, C.; Kasinrerk, W.; Malasit, P.; Atkinson, J.P.; Diamond, M.S. Secreted NS1 of Dengue Virus Attaches to the Surface of Cells via Interactions with Heparan Sulfate and Chondroitin Sulfate E. *PLoS Pathog* **2007**, *3*, e183. <https://doi.org/10.1371/journal.ppat.0030183>.
34. Costa, S.M.; Azevedo, A.S.; Paes, M.V.; Sarges, F.S.; Freire, M.S.; Alves, A.M.B. DNA Vaccines against Dengue Virus Based on the Ns1 Gene: The Influence of Different Signal Sequences on the Protein Expression and Its Correlation to the Immune Response Elicited in Mice. *Virology* **2007**, *358*, 413–423. <https://doi.org/10.1016/j.virol.2006.08.052>.
35. Chen, H.-R.; Lai, Y.-C.; Yeh, T.-M. Dengue Virus Non-Structural Protein 1: A Pathogenic Factor, Therapeutic Target, and Vaccine Candidate. *J Biomed Sci* **2018**, *25*, 58. <https://doi.org/10.1186/s12929-018-0462-0>.
36. Glasner, D.R.; Puerta-Guardo, H.; Beatty, P.R.; Harris, E. The Good, the Bad, and the Shocking: The Multiple Roles of Dengue Virus Nonstructural Protein 1 in Protection and Pathogenesis. *Annu. Rev. Virol.* **2018**, *5*, 227–253. <https://doi.org/10.1146/annurev-virology-101416-041848>.
37. Jayathilaka, D.; Gomes, L.; Jeewandara, C.; Jayarathna, Geetha.S.B.; Herath, D.; Perera, P.A.; Fernando, S.; Wijewickrama, A.; Hardman, C.S.; Ogg, G.S.; et al. Role of NS1 Antibodies in the Pathogenesis of Acute Secondary Dengue Infection. *Nat Commun* **2018**, *9*, 5242. <https://doi.org/10.1038/s41467-018-07667-z>.
38. Carpio, K.L.; Barrett, A.D.T. Flavivirus NS1 and Its Potential in Vaccine Development. *Vaccines* **2021**, *9*, 622. <https://doi.org/10.3390/vaccines9060622>.
39. Schlesinger, J.J.; Brandriss, M.W.; Walsh, E.E. Protection of Mice against Dengue 2 Virus Encephalitis by Immunization with the Dengue 2 Virus Non-Structural Glycoprotein NS1. *J Gen Virol* **1987**, *68* ( Pt 3), 853–857. <https://doi.org/10.1099/0022-1317-68-3-853>.
40. Costa, S.M.; Paes, M.V.; Barreto, D.F.; Pinhão, A.T.; Barth, O.M.; Queiroz, J.L.S.; Armôa, G.R.G.; Freire, M.S.; Alves, A.M.B. Protection against Dengue Type 2 Virus Induced in Mice Immunized with a DNA Plasmid Encoding the Non-Structural 1 (NS1) Gene Fused to the Tissue Plasminogen Activator Signal Sequence. *Vaccine* **2006**, *24*, 195–205. <https://doi.org/10.1016/j.vaccine.2005.07.059>.
41. Amorim, J.H.; Diniz, M.O.; Cariri, F.A.M.O.; Rodrigues, J.F.; Bizerra, R.S.P.; Gonçalves, A.J.S.; De Barcelos Alves, A.M.; De Souza Ferreira, L.C. Protective Immunity to DENV2 after Immunization with a Recombinant NS1 Protein Using a Genetically Detoxified Heat-Labile Toxin as an Adjuvant. *Vaccine* **2012**, *30*, 837–845. <https://doi.org/10.1016/j.vaccine.2011.12.034>.
42. Gonçalves, A.J.S.; Oliveira, E.R.A.; Costa, S.M.; Paes, M.V.; Silva, J.F.A.; Azevedo, A.S.; Mantuano-Barradas, M.; Nogueira, A.C.M.A.; Almeida, C.J.; Alves, A.M.B. Cooperation between CD4<sup>+</sup> T Cells and Humoral Immunity Is Critical for Protection against Dengue Using a DNA Vaccine Based on the NS1 Antigen. *PLoS Negl Trop Dis* **2015**, *9*, e0004277. <https://doi.org/10.1371/journal.pntd.0004277>.
43. Beatty, P.R.; Puerta-Guardo, H.; Killingbeck, S.S.; Glasner, D.R.; Hopkins, K.; Harris, E. Dengue Virus NS1 Triggers Endothelial Permeability and Vascular Leak That Is Prevented by NS1 Vaccination. *Sci. Transl. Med.* **2015**, *7*. <https://doi.org/10.1126/scitranslmed.aaa3787>.
44. Azevedo, A.S.; Yamamura, A.M.Y.; Freire, M.S.; Trindade, G.F.; Bonaldo, M.; Galler, R.; Alves, A.M.B. DNA Vaccines against Dengue Virus Type 2 Based on Truncate Envelope Protein or Its Domain III. *PLoS ONE* **2011**, *6*, e20528. <https://doi.org/10.1371/journal.pone.0020528>.
45. Caufour, P.S.; Motta, M.C.A.; Yamamura, A.M.Y.; Vazquez, S.; Ferreira, I.I.; Jabor, A.V.; Bonaldo, M.C.; Freire, M.S.; Galler, R. Construction, Characterization and Immunogenicity of Recombinant Yellow Fever 17D-Dengue Type 2 Viruses. *Virus Research* **2001**, *79*, 1–14. [https://doi.org/10.1016/S0168-1702\(01\)00273-8](https://doi.org/10.1016/S0168-1702(01)00273-8).

46. Gao, G.; Wang, Q.; Dai, Z.; Calcedo, R.; Sun, X.; Li, G.; Wilson, J.M. Adenovirus-Based Vaccines Generate Cytotoxic T Lymphocytes to Epitopes of NS1 from Dengue Virus That Are Present in All Major Serotypes. *Human Gene Therapy* **2008**, *19*, 927–936. <https://doi.org/10.1089/hum.2008.011>.
47. Rothman, A.L.; Kurane, I.; Ennis, F.A. Multiple Specificities in the Murine CD4 $\zeta$  and CD8 $\zeta$  T-Cell Response to Dengue Virus. *J. VIROL.* **1996**, *70*.
48. Alves, A.M.B.; Costa, S.M.; Pinto, P.B.A. Dengue Virus and Vaccines: How Can DNA Immunization Contribute to This Challenge? *Front. Med. Technol.* **2021**, *3*, 640964. <https://doi.org/10.3389/fmedt.2021.640964>.
49. Pinto, P.B.A.; Assis, M.L.; Vallochi, A.L.; Pacheco, A.R.; Lima, L.M.; Quaresma, K.R.L.; Pereira, B.A.S.; Costa, S.M.; Alves, A.M.B. T Cell Responses Induced by DNA Vaccines Based on the DENV2 E and NS1 Proteins in Mice: Importance in Protection and Immunodominant Epitope Identification. *Front. Immunol.* **2019**, *10*, 1522. <https://doi.org/10.3389/fimmu.2019.01522>.
50. Welch, M.; Villalobos, A.; Gustafsson, C.; Minshall, J. You're One in a Googol: Optimizing Genes for Protein Expression. *J. R. Soc. Interface.* **2009**, *6*. <https://doi.org/10.1098/rsif.2008.0520.focus>.
51. Hanson, G.; Collier, J. Codon Optimality, Bias and Usage in Translation and mRNA Decay. *Nat Rev Mol Cell Biol* **2018**, *19*, 20–30. <https://doi.org/10.1038/nrm.2017.91>.
52. Parvathy, S.T.; Udayasuriyan, V.; Bhadana, V. Codon Usage Bias. *Mol Biol Rep* **2022**, *49*, 539–565. <https://doi.org/10.1007/s11033-021-06749-4>.
53. Narum, D.L.; Kumar, S.; Rogers, W.O.; Fuhrmann, S.R.; Liang, H.; Oakley, M.; Taye, A.; Sim, B.K.L.; Hoffman, S.L. Codon Optimization of Gene Fragments Encoding *Plasmodium Falciparum* Merzoite Proteins Enhances DNA Vaccine Protein Expression and Immunogenicity in Mice. *Infect Immun* **2001**, *69*, 7250–7253. <https://doi.org/10.1128/IAI.69.12.7250-7253.2001>.
54. Ko, H.-J.; Ko, S.-Y.; Kim, Y.-J.; Lee, E.-G.; Cho, S.-N.; Kang, C.-Y. Optimization of Codon Usage Enhances the Immunogenicity of a DNA Vaccine Encoding Mycobacterial Antigen Ag85B. *Infect Immun* **2005**, *73*, 5666–5674. <https://doi.org/10.1128/IAI.73.9.5666-5674.2005>.
55. Lin, C.-T.; Tsai, Y.-C.; He, L.; Calizo, R.; Chou, H.-H.; Chang, T.-C.; Soong, Y.-K.; Hung, C.-F.; Lai, C.-H. A DNA Vaccine Encoding a Codon-Optimized Human Papillomavirus Type 16 E6 Gene Enhances CTL Response and Anti-Tumor Activity. *J Biomed Sci* **2006**, *13*, 481–488. <https://doi.org/10.1007/s11373-006-9086-6>.
56. Zhu, Y.; Lu, F.; Dai, Y.; Wang, X.; Tang, J.; Zhao, S.; Zhang, C.; Zhang, H.; Lu, S.; Wang, S. Synergistic Enhancement of Immunogenicity and Protection in Mice against *Schistosoma Japonicum* with Codon Optimization and Electroporation Delivery of SjTPI DNA Vaccines. *Vaccine* **2010**, *28*, 5347–5355. <https://doi.org/10.1016/j.vaccine.2010.05.017>.
57. Li, K.; Gao, L.; Gao, H.; Qi, X.; Gao, Y.; Qin, L.; Wang, Y.; Wang, X. Codon Optimization and Woodchuck Hepatitis Virus Posttranscriptional Regulatory Element Enhance the Immune Responses of DNA Vaccines against Infectious Bursal Disease Virus in Chickens. *Virus Research* **2013**, *175*, 120–127. <https://doi.org/10.1016/j.virusres.2013.04.010>.
58. Latanova, A.A.; Petkov, S.; Kilpelainen, A.; Jansons, J.; Latyshev, O.E.; Kuzmenko, Y.V.; Hinkula, J.; Abakumov, M.A.; Valuev-Elliston, V.T.; Gomelsky, M.; et al. Codon Optimization and Improved Delivery/Immunization Regimen Enhance the Immune Response against Wild-Type and Drug-Resistant HIV-1 Reverse Transcriptase, Preserving Its Th2-Polarity. *Sci Rep* **2018**, *8*, 8078. <https://doi.org/10.1038/s41598-018-26281-z>.
59. Peng, S.; Ferrall, L.; Gaillard, S.; Wang, C.; Chi, W.-Y.; Huang, C.-H.; Roden, R.B.S.; Wu, T.-C.; Chang, Y.-N.; Hung, C.-F. Development of DNA Vaccine Targeting E6 and E7 Proteins of Human Papillomavirus 16 (HPV16) and HPV18 for Immunotherapy in Combination with Recombinant Vaccinia Boost and PD-1 Antibody. *mBio* **2021**, *12*, e03224–20. <https://doi.org/10.1128/mBio.03224-20>.
60. Azevedo, A.S.; Gonçalves, A.J.S.; Archer, M.; Freire, M.S.; Galler, R.; Alves, A.M.B. The Synergistic Effect of Combined Immunization with a DNA Vaccine and Chimeric Yellow Fever/Dengue Virus Leads to Strong Protection against Dengue. *PLoS ONE* **2013**, *8*, e58357. <https://doi.org/10.1371/journal.pone.0058357>.
61. Pinto, P.B.A.; Barros, T.A.C.; Lima, L.M.; Pacheco, A.R.; Assis, M.L.; Pereira, B.A.S.; Gonçalves, A.J.S.; Azevedo, A.S.; Neves-Ferreira, A.G.C.; Costa, S.M.; et al. Combination of E- and NS1-Derived DNA Vaccines: The Immune Response and Protection Elicited in Mice against DENV2. *Viruses* **2022**, *14*, 1452. <https://doi.org/10.3390/v14071452>.
62. Mauro, V.P.; Chappell, S.A. A Critical Analysis of Codon Optimization in Human Therapeutics. *Trends in Molecular Medicine* **2014**, *20*, 604–613. <https://doi.org/10.1016/j.molmed.2014.09.003>.
63. Sroubek, J.; Krishnan, Y.; McDonald, T.V. Sequence and Structure-Specific Elements of HERG mRNA Determine Channel Synthesis and Trafficking Efficiency. *FASEB J* **2013**, *27*, 3039–3053. <https://doi.org/10.1096/fj.12-227009>.
64. Bertalovitz, A.C.; Badhey, M.L.O.; McDonald, T.V. Synonymous Nucleotide Modification of the KCNH2 Gene Affects Both mRNA Characteristics and Translation of the Encoded hERG Ion Channel. *Journal of Biological Chemistry* **2018**, *293*, 12120–12136. <https://doi.org/10.1074/jbc.RA118.001805>.

65. Agashe, D.; Martinez-Gomez, N.C.; Drummond, D.A.; Marx, C.J. Good Codons, Bad Transcript: Large Reductions in Gene Expression and Fitness Arising from Synonymous Mutations in a Key Enzyme. *Molecular Biology and Evolution* **2013**, *30*, 549–560. <https://doi.org/10.1093/molbev/mss273>.
66. Tsai, C.-J.; Sauna, Z.E.; Kimchi-Sarfaty, C.; Ambudkar, S.V.; Gottesman, M.M.; Nussinov, R. Synonymous Mutations and Ribosome Stalling Can Lead to Altered Folding Pathways and Distinct Minima. *Journal of Molecular Biology* **2008**, *383*, 281–291. <https://doi.org/10.1016/j.jmb.2008.08.012>.
67. Spencer, P.S.; Siller, E.; Anderson, J.F.; Barral, J.M. Silent Substitutions Predictably Alter Translation Elongation Rates and Protein Folding Efficiencies. *Journal of Molecular Biology* **2012**, *422*, 328–335. <https://doi.org/10.1016/j.jmb.2012.06.010>.
68. Sander, I.M.; Chaney, J.L.; Clark, P.L. Expanding Anfinsen's Principle: Contributions of Synonymous Codon Selection to Rational Protein Design. *J. Am. Chem. Soc.* **2014**, *136*, 858–861. <https://doi.org/10.1021/ja411302m>.
69. Hu, S.; Wang, M.; Cai, G.; He, M. Genetic Code-Guided Protein Synthesis and Folding in Escherichia Coli. *Journal of Biological Chemistry* **2013**, *288*, 30855–30861. <https://doi.org/10.1074/jbc.M113.467977>.
70. Yu, C.-H.; Dang, Y.; Zhou, Z.; Wu, C.; Zhao, F.; Sachs, M.S.; Liu, Y. Codon Usage Influences the Local Rate of Translation Elongation to Regulate Co-Translational Protein Folding. *Molecular Cell* **2015**, *59*, 744–754. <https://doi.org/10.1016/j.molcel.2015.07.018>.
71. Döşkaya, M.; Kalantari-Dehaghi, M.; Walsh, C.M.; Hiszczyńska-Sawicka, E.; Davies, D.H.; Felgner, P.L.; Larsen, L.S.Z.; Lathrop, R.H.; Hatfield, G.W.; Schulz, J.R.; et al. GRA1 Protein Vaccine Confers Better Immune Response Compared to Codon-Optimized GRA1 DNA Vaccine. *Vaccine* **2007**, *25*, 1824–1837. <https://doi.org/10.1016/j.vaccine.2006.10.060>.
72. Dobaño, C.; Sedegah, M.; Rogers, W.O.; Kumar, S.; Zheng, H.; Hoffman, S.L.; Doolan, D.L. Plasmodium: Mammalian Codon Optimization of Malaria Plasmid DNA Vaccines Enhances Antibody Responses but Not T Cell Responses nor Protective Immunity. *Experimental Parasitology* **2009**, *122*, 112–123. <https://doi.org/10.1016/j.exppara.2009.02.010>.
73. Imani Fooladi, A.A.; Bagherpour, G.; Khoramabadi, N.; Fallah Mehrabadi, J.; Mahdavi, M.; Halabian, R.; Amin, M.; Izadi Mobarakeh, J.; Einollahi, B. Cellular Immunity Survey against Urinary Tract Infection Using pVAX/ *Fim* H Cassette with Mammalian and Wild Type Codon Usage as a DNA Vaccine. *Clin Exp Vaccine Res* **2014**, *3*, 185. <https://doi.org/10.7774/cevr.2014.3.2.185>.

**Disclaimer/Publisher's Note:** The statements, opinions and data contained in all publications are solely those of the individual author(s) and contributor(s) and not of MDPI and/or the editor(s). MDPI and/or the editor(s) disclaim responsibility for any injury to people or property resulting from any ideas, methods, instructions or products referred to in the content.